CHEMISTRY
A EUROPEAN JOURNAL

DOI: 10.1002/chem.200801061

Ruthenium Complexes of Substituted Hydrazine: New Solution- and Solid-State Binding Modes

Serin L. Dabb,[a] Barbara A. Messerle,*[a] Gottfried Otting,[b] Jörg Wagler,[c] and Anthony Willis[b]

Abstract: The methylhydrazine complex $[Ru(NH_2NHMe)(PyP)_2]Cl(BPh_4)$ (PyP = 1-[2-(diphenylphosphino)ethyl]-pyrazole) was synthesised by addition of methylhydrazine to the bimetallic complex $[Ru(\mu\text{-}Cl)(PyP)_2]_2(BPh_4)_2$. The methylhydrazine ligand of the ruthenium complex has two different binding modes: side-on (η^2-) when the complex is in the solid state and end-on (η^1-) when the complex is in solution. The solid-state structure of $[Ru(PyP)_2(NH_2NHMe)]Cl(BPh_4)$ was determined by X-ray crystallography. 2D NMR spectroscopic experiments with ^{15}N at natural abundance confirmed that in solution the methylhydrazine is bound to the metal centre by only the -NH_2 group and the ruthenium complex retains an octahedral conformation. Hydrazine complexes $[RuCl(PyP)_2(\eta^1\text{-}NH_2NRR')]OSO_2CF_3$ (in which R = H, R′ = Ph, R = R′ = Me and NRR′ = NC_5H_{10}) were formed in situ by the addition of phenylhydrazine, 1,1-dimethylhydrazine and *N*-aminopiperidine, respectively, to a solution of the bimetallic complex $[Ru(\mu\text{-}Cl)(PyP)_2]_2(OSO_2CF_3)_2$ in dichloromethane. These substituted hydrazine complexes of ruthenium were shown to exist in an equilibrium mixture with the bimetallic starting material.

Keywords: coordination modes · hydrazine · NMR spectroscopy · ruthenium · X-ray diffraction

Introduction

The chemistry of metal-coordinated hydrazine and substituted hydrazines has been extensively studied, primarily because of the potential significance of coordinated hydrazine in the reaction pathways of organometallic nitrogen-reducing systems.[1–3] The biological reduction of N_2 to ammonia is mediated by three main types of nitrogenase enzymes that contain metal clusters of Fe, V and Mo at their active sites,[4] and iron is the only metal common to all nitrogenase enzymes. The industrial reduction of N_2, which uses the Haber–Bosch process, also relies on an iron- or ruthenium-based catalyst.[5] The significance of iron and ruthenium in these two processes underlines the importance of Group 8 metal centres in the reduction of N_2 to ammonia and has sparked much interest in the synthesis of hydrazine and diazine complexes of Fe, Ru and Os.[6–13]

There are two possible binding modes of hydrazine and substituted hydrazines with a single metal centre: either η^2- (side-on, bidentate) or η^1- (end-on, monodentate), which is the most common. Without X-ray crystallography, it is difficult to predict whether mono-substituted hydrazines preferentially coordinate to the metal centre by the substituted β- or unsubstituted α-nitrogen because of competing steric and electronic effects. Structure determination by X-ray crystallography has shown that the majority of known hydrazine complexes contain substituted hydrazines bound by the α-nitrogen.[6]

NMR spectroscopy can be used to analyze the stereochemistry and nature of hydrazine binding in metal complexes of hydrazine in solution.[6,14,15] The most important NMR spectroscopy parameters for such structural characterisation are the Overhauser effect and scalar coupling constants. NMR spectroscopic experiments have been developed previously for the sensitive detection of these NMR parameters for compounds that contain a natural abundance

[a] Dr. S. L. Dabb, Prof. B. A. Messerle
School of Chemistry
The University of New South Wales
Sydney, NSW 2052 (Australia)
Fax: (+61) 2-9385-6141
E-mail: b.messerle@unsw.edu.au

[b] Prof. G. Otting, Dr. A. Willis
Research School of Chemistry
The Australian National University
Canberra, ACT 0200 (Australia)

[c] Dr. J. Wagler
Institut für Anorganische Chemie
TU Bergakademie Freiberg
Leipziger Str. 29
09596 Freiberg (Germany)

of ^{15}N nuclei, but have not been widely applied to the analysis of metal complexes of hydrazine.[16–18] The use of these techniques can alleviate the expense of using ^{15}N-labelled hydrazines and provide an alternative to X-ray crystallography for stereochemical analysis.

There are a very limited number of reported metal complexes that contain a bidentate hydrazine ligand or substituted hydrazine ligand. The first X-ray crystal structure obtained for a bidentate hydrazine ligand, η^2-NH_2NH_2, was of a cobalt complex that contained a tripodal P donor ligand, $[Co(CH_3C(CH_2PPh_2)_3)(\eta^2\text{-}NH_2NH_2)](BPh_4)_2$.[19] Tungsten and molybdenum complexes of η^2-hydrazines, such as $[WCp^*(Me_3)(\eta^2\text{-}NH_2NH_2)]OSO_2CF_3$[20] (**1**) and $[MoCpI(\eta^2\text{-}NHPhNH_2)(NO)]BF_4$[21] (**2**), have also been structurally characterised. It has been postulated that a series of hydrazine complexes with a similar structure to tungsten complex **1**, $[MCp^*(Me_3)(\eta^2\text{-}NH_2NH_xMe_{2-x})]OSO_2CF_3$ (in which M = Mo,[22] W[23] or Re[24] and $x = 0$–2), also have the hydrazine ligand bound in a side-on fashion. Group 5 metal complexes of 1,1-disubstituted η^2-hydrazines, such as $[VCl_2(\eta^2\text{-}H_2NNMePh)_2(NNMePh)]Cl$,[25] have also been structurally characterised.[25,26] Although there are limited examples of the η^2 binding mode of hydrazine and substituted hydrazine, the potential is that such a binding mode might activate the hydrazine unit towards reactivity with organic species or cleavage of the N–N bond to a greater extent than is observed in the η^1-hydrazine complexes.

The first syntheses of Group 8 metal complexes that contain a bidentate hydrazine ligand have only recently been reported.[27,28] The hydrazine complexes *cis*-$[Fe(\eta^2\text{-}NH_2NH_2)(\widehat{PP})_2](BPh_4)_2$, in which $\widehat{PP}$ = 1,2-bis[bis-(methoxypropyl)phosphino]ethane (**3**) or 1,2-bis(dimethylphosphino)ethane (**4**), were synthesised from the dichloride iron precursor $[FeCl_2(\widehat{PP})_2]$, hydrazine and two equivalents of $NaBPh_4$ (Scheme 1).[27,28]

The work reported here describes the synthesis and characterisation of the first example of a substituted-hydrazine complex of ruthenium in which the methylhydrazine ligand assumes both a monodentate and bidentate coordination mode (Scheme 2).

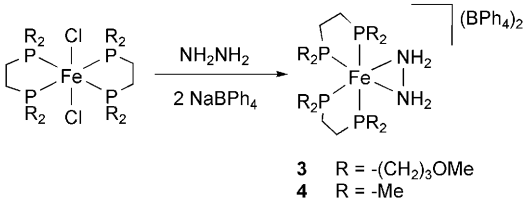

Scheme 1. Synthesis of complexes **3** and **4**.

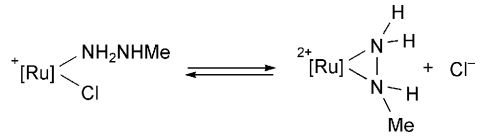

Scheme 2. The two possible binding modes of methylhydrazine.

Results and Discussion

Synthesis and reactivity of $[Ru(NH_2NHMe)(PyP)_2]Cl(BPh_4)$ (5; PyP = 1-[2-(diphenylphosphino)ethyl]pyrazole): The reaction of methylhydrazine with ruthenium dimer $[Ru(\mu\text{-}Cl)(PyP)_2]_2(BPh_4)_2$ (**6**)[29] gave new Ru hydrazine complex **5** as either $[Ru(\eta^2\text{-}NH_2NHMe)(PyP)_2]Cl(BPh_4)$ (**5a**) in which the hydrazine acts as a bidentate ligand, or $[RuCl(\eta^1\text{-}NH_2NHMe)(PyP)_2]BPh_4$ (**5b**) in which the hydrazine is bound in an end-on fashion by the $-NH_2$ group (Scheme 3).

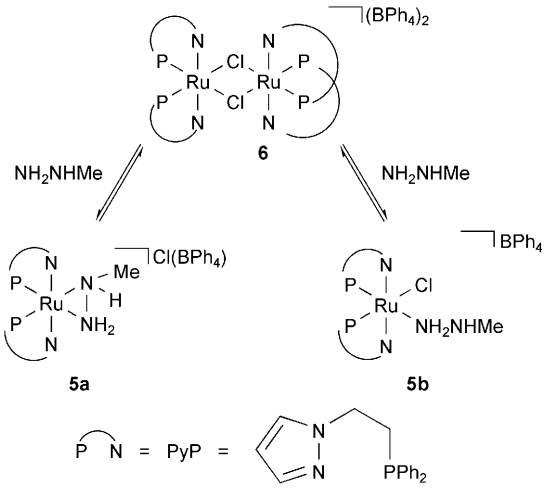

Scheme 3. Synthesis of **5** from **6**, showing the structures of **5a** (side-on binding of methylhydrazine) and **5b** (end-on binding of methylhydrazine).

The reaction was performed at room temperature in dichloromethane and gave **5** cleanly and in good yield (68%); the reaction did not proceed at −30 °C. Complex **6** was synthesised by heating a solution of *trans*,*cis*,*cis*-$[RuCl_2(PyP)_2]$ and $NaBPh_4$ in ethanol at reflux, thereby following the reported method.[29]

Loss of methylhydrazine from **5** in solution led to the formation of starting material **6**, which precipitated out of solutions of **5** in tetrahydrofuran, chloroform and dichloromethane. The tendency of **5** to lose methylhydrazine meant there was little potential for undertaking further reactions of the metal-bound hydrazine ligand.

Given the reversibility of hydrazine addition, it was thought that the greater solubility of bimetallic Ru complex $[Ru(\mu\text{-}Cl)(PyP)_2]_2(OSO_2CF_3)_2$ (**7**),[29] which contains a triflate counterion, would lead to an increase in the stability of proposed product $[Ru(NH_2NHMe)(PyP)_2]Cl(OSO_2CF_3)$ (**8**) by addition of methylhydrazine. Unfortunately, addition of methylhydrazine to a solution of **7** in dichloromethane produced a number of products including the expected complex **8**, as observed by $^{31}P\{^1H\}$ and ^1H NMR spectroscopy.

Crystals of **5a** were successfully grown by layering *n*-hexane over a solution of **5** in tetrahydrofuran and a slight excess of methylhydrazine. The excess methylhydrazine was needed to prevent the preferential precipitation of BPh_4^-

dimer **6**. Early attempts to grow crystals from solutions of **5** and methylhydrazine in dichloromethane resulted in the formation of 1,4-dimethylhexahydro-1,2,4,5-tetrazine (**9**). Tetrazine **9** is intentionally synthesised by heating methylhydrazine and dichloromethane in diethyl ether at 34 °C for several hours.[30]

Solid-state structure of 5: The solid-state structure of **5** was confirmed by X-ray crystallography to be **5a**. The ORTEP diagram that shows the atomic numbering scheme for **5a** is shown in Figure 1. Selected bond lengths and angles for the solid-state structure of **5a** are presented in Table 1.

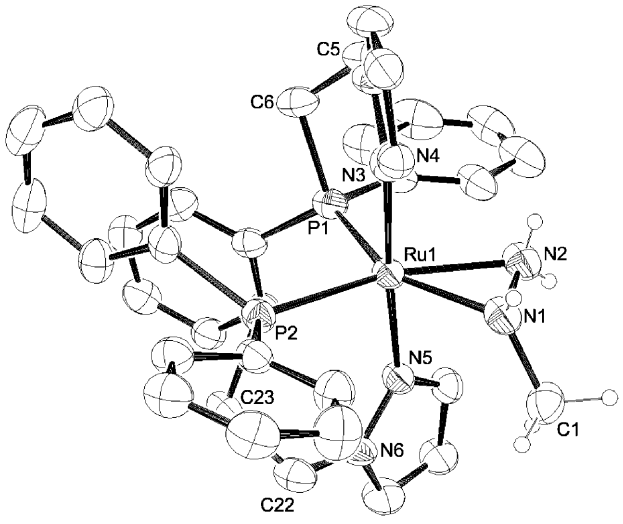

Figure 1. ORTEP depiction of the cation of **5a**, with thermal ellipsoids at the 30% probability level. All H atoms except those of the methylhydrazine ligand have been omitted for clarity.

Table 1. Selected bond lengths and angles for the solid-state structure of **5a**.

Bond lengths [Å]		Bond angles [°]	
Ru1–N1	2.147(6)	N1-Ru1-N2	39.1(2)
Ru1–N2	2.110(6)	N3-Ru1-P1	95.02(15)
Ru1–N3	2.107(5)	N3-Ru1-N5	174.99(19)
Ru1–N5	2.104(5)	N5-Ru1-P2	92.64(14)
Ru1–P1	2.275(2)	P1-Ru1-P2	92.79(6)
Ru1–P2	2.273(2)		
N1–N2	1.423(9)		

The asymmetric unit of the crystal structure obtained for **5a** consists of one molecule of **5a**, (the crystal lattice clearly shows that both Cl^- and BPh_4^- anions are present), 1.5 molecules of methylhydrazine and one molecule of tetrahydrofuran.

The geometry about the ruthenium metal centre of **5a** is pseudo-octahedral, in which the methylhydrazine ligand occupies two equatorial sites. The severe distortion from ideal octahedral geometry is caused by the methylhydrazine ligand, in which the N1-Ru1-N2 bite angle is only 39.1(2)°. The angle between the plane occupied by P1-Ru-P2 and the plane occupied by N1-Ru1-N2 is 2.9(0.4)°. The Ru–P and Ru–N bond lengths and N-Ru-P bite angles of the PyP ligands bound to **5a** are all comparable to those found for previously reported ruthenium complexes that contain two PyP ligands.[29] The bond lengths for N1–N2, Ru1–N1 and Ru1–N2 (1.423(9), 2.147(6) and 2.110(6) Å, respectively) are all within the ranges of Ru–N and N–N bond lengths found for previously reported ruthenium complexes that contain η^1-hydrazine ligands[10,11,31] and Fe, Co, V, W and Mo complexes **1**–**4**, which contain bidentate hydrazine ligands.[19–21,25,27]

Although close to the limit of experimental error, the Ru1–N1 bond (2.147(6) Å) of the methylhydrazine ligand is slightly longer than the Ru1–N2 bond (2.110(6) Å), which indicates that the $-NH_2$ group of the methylhydrazine ligand binds more strongly to the metal centre than the alkyl-substituted nitrogen, -NHMe. This is of note because no conclusive data has been previously reported that distinguishes between the binding strengths of the α- and β-nitrogen atoms of alkyl-substituted hydrazines.[6] A previous report on **2**, a molybdenum complex that contains the aryl-substituted hydrazine ligand η^2-phenylhydrazine, also found the Mo–NHPh bond (2.184(3) Å) to be longer than the Mo–NH_2 bond (2.134(3) Å), as determined by X-ray crystallography.[21]

Solution-state structure of 5: Extensive NMR spectroscopic studies showed that in solution the methylhydrazine ligand of **5** was bound in an end-on fashion by the $-NH_2$ group as in **5b**. ^{1}H-^{1}H NOESY, ^{1}H-^{1}H ROESY and ^{1}H-^{1}H DQF-COSY experiments were performed to assign the resonances of the protons in the ^{1}H NMR spectrum of **5b**. The three resonances due to the NH signals of the methylhydrazine ligand appear as broad multiplets at three separate chemical shifts that integrate to one proton each. The signals were assigned by using the ^{1}H-^{1}H DQF-COSY spectrum, which contains cross peaks between the resonances from the methyl protons of the methylhydrazine and the -NHMe proton, and cross peaks between the resonances from the protons bound to the two nitrogen atoms of methylhydrazine.

The geometry of the first coordination sphere of the Ru ion was assessed by two-bond scalar coupling constants across the metal centre. The octahedral geometry of the Ru ion coordinated by PyP ligands, which was observed in the crystal structure, appears to be conserved in solution. The ^{31}P{^{1}H} NMR spectrum showed a pair of doublets at $\delta = 38.8$ and 28.7 ppm (^2J(P,P) = 30 Hz; Figure 5b, later). This splitting pattern is consistent with a coupled pair of inequivalent phosphorus nuclei that are *cis* to each other, as expected for **5a** or **5b**. In addition, the absence of any large ^2J(P,N) couplings of the PyP nitrogen atoms in a ^{1}H-^{15}N HSQC spectrum (recorded with INEPT delays of 25 ms) indicated that none of the PyP nitrogen atoms were *trans* to a phosphorus atom, which confirms the geometry of the compound as either **5a** or **5b**.

A ^{1}H-^{15}N HSQC spectrum recorded with INEPT delays of 6.7 ms provided experimental evidence for the end-on co-

ordination of the methylhydrazine ligand to the metal centre by only the NH_2 group. Sections of the ^1H-^{15}N HSQC spectrum are shown in Figure 2. As can be seen from the

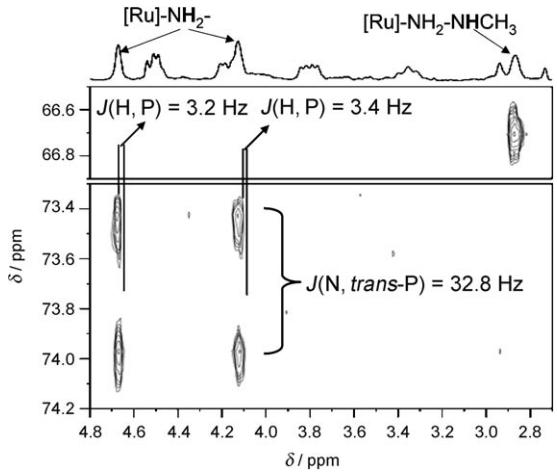

Figure 2. Sections of the ^1H-^{15}N HSQC spectrum ($CDCl_3$, 600 MHz) of **5b**, referenced externally to liquid ammonia.

2D spectrum, the ^{15}N resonance due to the methyl-substituted nitrogen appears as a singlet at $\delta = 66.7$ ppm, and the resonance due to the -NH_2 nitrogen appears as a doublet at $\delta = 73.7$ ppm. The large ^2J(N,P) coupling constant (32.8 Hz) of the -NH_2 nitrogen is indicative of a nitrogen atom *trans* to phosphorus. No such ^2J(N,P) coupling to phosphorus was observed for the -NHMe nitrogen resonance, which indicates that this nitrogen is not bound to ruthenium. The large ^2J(N,P) coupling constant observed for the -NH_2 nitrogen also confirms that the molecule has maintained its octahedral geometry, with a single phosphorus atom *trans* to the methylhydrazine ligand. The other phosphorus atom is most likely *trans* to a chloride anion. The J(N,P) coupling between the unsubstituted nitrogen and the *cis*-phosphines could not be resolved, even with ^{15}N linewidths less than 2.8 Hz, in agreement with ^2J(N,*cis*-P) couplings smaller than 3 Hz in octahedrally coordinated Ru complexes.[17,18] As expected, the ^3J(P,H) couplings between the two -NH_2 protons and the *trans*-phosphorus atoms were also small (^3J(P,H) = 3.2 and 3.4 Hz, Figure 2).

The sixth coordination site of the Ru ion is most likely occupied by the chloride anion with weak binding affinity. Indirect evidence for this was obtained from chemical exchange peaks between the signals of the two non-equivalent PyP ligands observed in the ROESY spectrum. The exchange rate was about 5 s^{-1} at 25 °C and changed little at 4 °C. The most plausible mechanism would be the dissociation of the chloride ion from the complex followed by migration of the methylhydrazine ligand to the vacant site and reassociation of the chloride ion. This mechanism would exchange the two PyP ligands without changing the coordination geometry of the methylhydrazine or the chirality of the complex.

A second exchange process was observed between the three nitrogen-bound protons of the methylhydrazine. This exchange process could be efficiently suppressed by lowering the temperature to 4 °C. These protons also showed exchange peaks to a resonance at $\delta = 1.53$ ppm, and this is most readily explained by intermolecular exchange with water.

There are only a few reported examples of ^{15}N NMR spectroscopic data for metal complexes of hydrazine, particularly for those of the later transition metals, such as ruthenium.[6] Relevant examples are given in Table 2. The chemical shifts of the resonances due to the nitrogen atoms of the methylhydrazine ligand are similar to those found for the rhodium complex [RhCl(η^1-NH_2NHMe)(PPh_3)$_2$], which also contains the methylhydrazine bound in an end-on fashion by the -NH_2 group *trans* to a phosphorus atom (Entry 2, Table 2).[14] The resonance due to the unsubstituted nitrogen (α-N) of methylhydrazine shifts noticeably downfield on binding to the ruthenium metal centre of **5b** (from $\delta = 51.2$ to 73.7 ppm), unlike the resonance due to the substituted nitrogen (β-N), which does not shift significantly. Similar shifts are also observed for [RhCl(η^1-NH_2NHMe)(PPh_3)$_2$].[14] These results further confirm that the β-N of the methylhydrazine ligand of **5b** is not bound to the metal centre. The chemical shifts of the resonances due to the nitrogen atoms of the end-on bound methylhydrazine ligands (Entries 2 and 5, Table 2) are significantly different to those of the bidentate hydrazine ligand of [Fe($\widehat{PP}$)$_2$(η^2-NH_2NH_2)](BPh_4)$_2$ (**3** and **4**; Entries 3 and 4, Table 2).[27] The ^{15}N chemical shifts may thus present a useful diagnostic tool for distinguishing the two different binding modes of hydrazine ligands.

Table 2. ^{15}N chemical shifts for free and ligated hydrazines, referenced to liquid ammonia.[a]

Entry	Compound	$\delta_{\alpha\text{-N}}$ [ppm]	$\delta_{\beta\text{-N}}$ [ppm]
1[14]	NH_2–NHMe	51.2[b]	64.2[b]
2[14]	[RhCl(η^1-NH_2NHMe)(PPh_3)$_2$]	68.1[b]	63.6[b]
3[27]	**3**	−13.1[c]	–
4[28]	**4**	−7.7[b]	–
5	**5b**	73.7	66.7

[a] α-N: unsubstituted nitrogen, β-N: substituted nitrogen. [b] Values of $\delta_{^{15}N}$ with respect to nitromethane have been converted to $\delta_{^{15}N}$ with respect to liquid NH_3 by using $\delta_{^{15}NH_3} = \delta_{Me^{15}NO_2} + 380.2$ ppm.[32,33] [c] Value is incorrectly referenced in original paper[27] in regards to $\delta_{^{15}N\ formamide}$,[33] and has been adjusted.

The ^1H-^1H ROESY spectrum also confirmed that the methylhydrazine ligand of **5b** is bound to the metal centre by only the -NH_2 group. ^1H-^1H ROESY was used instead of ^1H-^1H NOESY for determining the through-space interactions of the resonances of the protons of **5b** because the rotational correlation time of the complex led to much more intense ROE than NOE cross peaks.[35] Sections of the ^1H-^1H ROESY NMR spectrum are shown in Figures 3 and 4.

The two protons on the unsubstituted α-NH_2 of methylhydrazine are magnetically inequivalent, and both exhibit

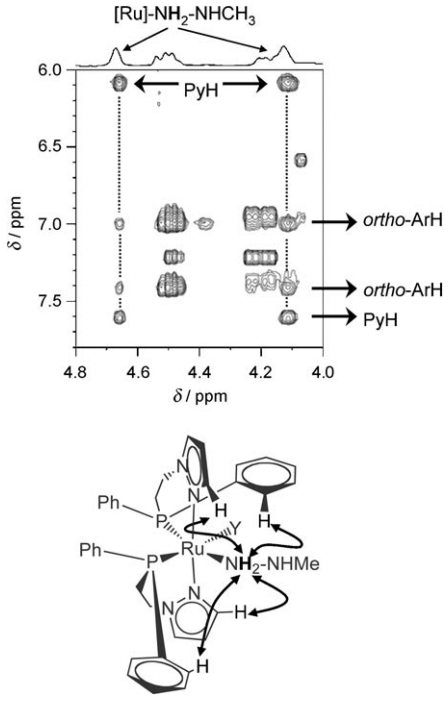

Figure 3. Section of the ^{1}H-^{1}H ROESY spectrum ($CDCl_3$, 600 MHz, 200 ms mixing time) and a pictorial depiction of the structure of **5b** that shows the through-space interactions of the protons of the ligands (PyH = pyrazolyl-H, ArH = aryl-H).

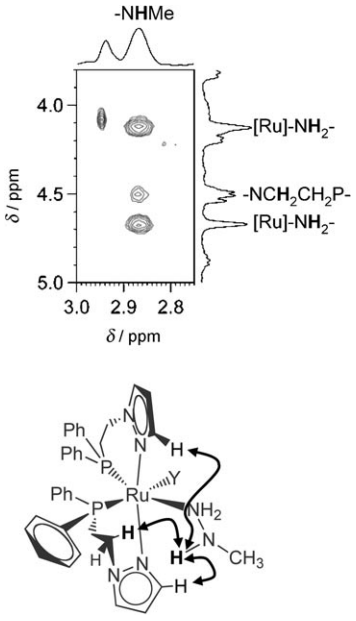

Figure 4. Section of the ^{1}H-^{1}H ROESY spectrum ($CDCl_3$, 600 MHz, 200 ms mixing time) and a pictorial depiction of the structure of **5b** that shows the through-space interactions of the protons of the ligands.

through-space interactions with the protons of the two inequivalent PyP ligands. ROESY cross peaks were observed between the ^{1}H NMR resonances of the α-NH protons and the protons on the C5 position of the pyrazole group of both PyP ligands, and those in the *ortho* positions of one of the phenyl groups of both PyP ligands (Figure 3). The resonances of both α-NH protons seem to exhibit through-space interactions with protons of both PyP ligands, even though the two pyrazole groups and two phenyl groups are oriented on opposite sides of the molecule. This observation is most readily explained by exchange-relayed ROEs, in which the weaker set of cross peaks arises from two-step magnetization transfers that involve both ROE and chemical exchange.

The section of the ^{1}H-^{1}H ROESY spectrum shown in Figure 4 shows the cross peak between the resonance due to the β-NH proton of methylhydrazine and one of the protons of the ethylene backbone, -NCH_2-, of one of the PyP ligands. This -NCH_2- group most likely belongs to the PyP ligand, the P and N donor atoms of which are both bound to the metal centre in a *cis* fashion to the methylhydrazine ligand (see the pictorial representation in Figure 4). This through-space interaction would not be possible if the β-N was bound to the ruthenium centre because the β-N would then be bound *trans* to the P donor atom of this PyP ligand. Cross peaks were also observed between the resonances of the β-NH proton and the protons on the C5 position of the pyrazole group of both PyP ligands.

The ^{1}H-^{31}P HMQC spectrum confirmed the orientation of the two PyP ligands of **5b**. A cross peak was observed between the resonances of one of the α-NH protons of methylhydrazine and the *trans*-^{31}P nucleus at $\delta = 28.7$ ppm. No cross peak was observed between the resonances due to the α-NH protons and the *cis*-^{31}P nucleus, which is expected because no ^{2}J(N,P) couplings could be resolved between the methylhydrazine nitrogen atoms and the *cis*-phosphines in the ^{1}H-^{15}N HSQC spectrum (Figure 2).

In situ synthesis of ruthenium complexes of hydrazine: Following the success of the reaction between methylhydrazine and ruthenium bimetallic complexes **6** and **7**, the scope of the reaction was extended to include less reactive substituted hydrazines. The in situ reaction of phenylhydrazine, 1,1-dimethylhydrazine, *N*-aminopiperidine and 1,2-diphenylhydrazine with **7** were first performed on an NMR scale. In each case, excess substituted hydrazine was added to a solution of dimer **7** in [D_2]dichloromethane and the reaction monitored by variable temperature ^{31}P{^{1}H} NMR spectroscopy. The addition of methylhydrazine to **6** gave the product with an end-on bound methylhydrazine ligand in solution, so therefore the products of the reactions between phenylhydrazine, 1,1-dimethylhydrazine and *N*-aminopiperidine with **7** were expected to be [$RuCl(\eta^1$-$NH_2NRR')$-$(PyP)_2]OSO_2CF_3$, in which R = H, R′ = Ph (**10**), R = R′ = Me (**11**) and NRR′ = NC_5H_{10} (**12**), respectively (Scheme 4).

Upon addition of phenylhydrazine to **7**, product **10** was formed immediately and exhibited a pair of doublets in the ^{31}P{^{1}H} NMR spectrum at $\delta = 44.3$ and 33.4 ppm (^{2}J(P,P) = 33.7 Hz; Figure 5c). Treatment of **7** with 1,1-dimethylhydrazine and *N*-aminopiperidine also produced new complexes **11** and **12**, which both exhibited a pair of doublets in their ^{31}P{^{1}H} NMR spectra, but at lower chemical shifts than the

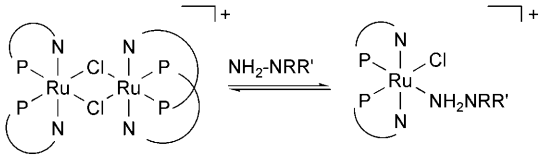

Scheme 4. Synthesis of complexes **10**–**12** from starting materials **6** or **7**, showing the end-on binding mode of the substituted hydrazines.

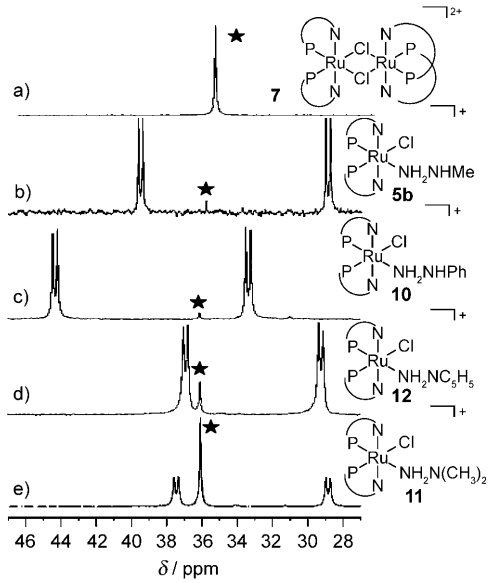

Figure 5. $^{31}P\{^1H\}$ NMR spectrum (250 K, 300 MHz) of a) **7** (★) in CD_2Cl_2; b) **5b** in $CDCl_3$; c), d) and e) **7** and excess **10**, **12** and **11**, respectively, in CD_2Cl_2.

mono-substituted hydrazine ($\delta = 37.5$ and 28.9 ppm for **11** and $\delta = 36.9$ and 29.3 ppm for **12**). The ^{31}P nuclei of each of the new complexes **10**–**12** have similar $^2J(P,P)$ coupling constants (33.7, 29.4 and 30.0 Hz, respectively; Figure 5). This splitting pattern is consistent with each complex containing mutually inequivalent P donor atoms that are *cis* to each other. The $^{31}P\{^1H\}$ NMR spectra of these three reaction mixtures, starting material **7** and isolated complex **5b** are depicted in Figure 5. The similarity of the chemical shifts and coupling constants of the in situ-formed hydrazine complexes of ruthenium to those of isolated complex **5b** confirm that substituted hydrazines phenylhydrazine, 1,1-dimethylhydrazine and *N*-aminopiperidine also give ruthenium complexes with the hydrazine ligand coordinated by the $-NH_2$ group in an end-on fashion, as depicted in Scheme 4.

The in situ reactions of phenylhydrazine with each of the dimers **6**, $[Ru(\mu\text{-}Cl)(PyP)_2]_2(BF_4)_2$ and $[Ru(\mu\text{-}Cl)(PyP)_2]_2(BArF)_2$ (in which BArF = tetrakis[3,5-bis(trifluoromethyl)phenyl]borate) were also performed on an NMR scale and monitored by low-temperature $^{31}P\{^1H\}$ NMR spectroscopy. The product of each of the three reactions had $^{31}P\{^1H\}$ NMR spectra that were similar to that observed for the reaction of phenylhydrazine with **7**, which contains a triflate counterion and was used in the formation of **10**–**12** (Figure 5c).

In the reactions of phenylhydrazine, 1,1-dimethylhydrazine and *N*-aminopiperidine with **7**, the new hydrazine products formed (**10**–**12**) were found to be in equilibrium with starting material **7**, even at low temperatures (190 K) and even though an excess of the hydrazine was used (note the residual peak attributed to **7** in each of the spectra in Figure 5c, d and e). This indicates that the substituted hydrazines are weakly bound to the metal centre, which is also confirmed by the broad resonances observed in the NMR spectra at room temperature. The reaction with phenylhydrazine produced much sharper resonances in the $^{31}P\{^1H\}$ NMR spectra at higher temperatures (270–298 K) than the reactions with the two 1,1-disubstitued hydrazines, which indicates that **10** is less labile than **11** and **12**.

1,2-diphenylhydrazine showed no reactivity towards **7** as observed by $^{31}P\{^1H\}$ NMR spectroscopy, even after 24 h at room temperature and a further 2 h at 60 °C. This is most likely due to the steric bulk of the phenyl group and the fact that the -NHPh nitrogen is less nucleophilic than the $-NH_2$ nitrogen of phenylhydrazine because of the delocalisation of electron density onto the aromatic ring. The fact that phenylhydrazine binds to ruthenium whereas 1,2-diphenylhydrazine does not supports the conclusion that the substituted hydrazine ligands bind in an end-on fashion in solution by the $-NH_2$ group.

Conclusion

Methylhydrazine complex **5** was synthesised by the addition of methylhydrazine to dimeric species **6**. The methylhydrazine ligand of **5** has two different binding modes, that is, side-on when complex **5** is in the solid state (**5a**) and end-on by the NH_2 group only when complex **5** is in solution (**5b**). The solid-state structure of **5** was determined by X-ray crystallography and the solution-state structure of **5** was determined by using 2D NMR spectroscopy. ^1H-^{15}N HSQC experiments provided particularly clear evidence that methylhydrazine is bound to the metal centre by only the $-NH_2$ group and that the ruthenium complex retains an octahedral conformation in solution. It is proposed here that the sixth vacant coordination site is filled by a chloride anion.

Hydrazine complexes $[RuCl(\eta^1\text{-}NH_2NRR')(PyP)_2]OSO_2CF_3$, in which R = H, R′ = Ph (**10**), R = R′ = Me (**11**) and NRR′ = NC_5H_{10} (**12**), were formed in situ by the addition of phenylhydrazine, 1,1-dimethylhydrazine and *N*-aminopiperidine, respectively, to a solution of **7** in dichloromethane. Complexes **10**–**12** were observed in an equilibrium mixture with dimeric ruthenium starting material **7**.

Experimental Section

All reactions were performed under a N_2 or Ar atmosphere. Solvents and liquid reagents were purified and dried under Ar by using conventional

methods.[36] Except where specified, chemicals were purchased from either Aldrich Chemical Company, Precious Metals Online PMO P/L or Cambridge Isotope Laboratory. The ^{1}H, ^{31}P and ^{13}C NMR spectra were recorded by using Bruker DPX300, DMX500, DMX600 or Avance 600 NMR spectrometers. ^{1}H and ^{13}C NMR chemical shifts were referenced internally to residual solvent resonances. ^{31}P NMR chemical shifts were referenced externally by using H_3PO_4 (85% in D_2O) in a capillary that was taken to be at 0.0 ppm. ^{15}N NMR chemical shifts were referenced externally to liquid ammonia, which was taken to be at 0 ppm. The ^{1}H-^{15}N HSQC spectrum of Figure 2 was recorded with broadband ^{1}H decoupling during the evolution time to minimize the ^{15}N linewidth in the presence of ^{1}H chemical exchange.[37] Elemental analyses were carried out at the Campbell Microanalytical Laboratory, University of Otago, New Zealand. Single-crystal X-ray diffraction data were collected in ϕ and ω scans by using a Nonius Kappa CCD diffractometer with $Mo_{K\alpha}$ radiation. The structures were solved with direct methods (SHELXS97) and refined by full-matrix least-squares refinement of F^2 by using SHELXL97. Details of crystallographic data for compound **5** are listed in the experimental section. CCDC-689122 (**5**) contains the supplementary crystallographic data for this paper. These data can be obtained free of charge from The Cambridge Crystallographic Data Centre via www.ccdc.cam.ac.uk/data_request/cif. Mass spectra were acquired at the BioAnalytical Mass Spectrometry Facility (BMSF), University of New South Wales. Complexes **6**, **7**, $[Ru(\mu\text{-}Cl)(PyP)_2]_2(BF_4)_2$ and $[Ru(\mu\text{-}Cl)(PyP)_2]_2(BArF)_2$ were synthesised by following the reported methods.[29]

Synthesis of $[Ru(NH_2NHMe)(PyP)_2]Cl(BPh_4)$ (5): Methylhydrazine (50 μL, 0.950 mmol) was added to a solution of **6** (74.7 mg, 0.037 mmol) in CH_2Cl_2 (10 mL). The solution was stirred for 1 h, then concentrated under vacuum and Et_2O added. The subsequent precipitate was collected by filtration and dried under vacuum to give the title product as a pale yellow solid (yield 53.6 mg, 68%). Crystals suitable for X-ray crystallography were grown by layering *n*-hexane over a solution of methylhydrazine and the crude product in THF.

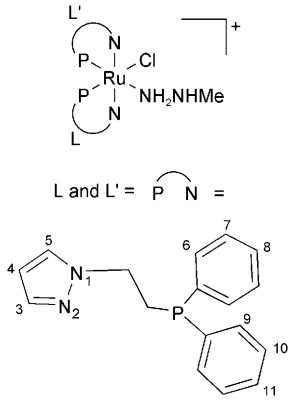

^{1}H NMR (600 MHz, $CDCl_3$, 298 K, TMS): δ = 7.60 (1H; **H**3), 7.41 (2H; **H**′9), 7.38 (1H; **H**11), 7.36 (8H; *o*-C**H** of BPh_4), 7.31 (2H; **H**10), 7.28 (1H; **H**′11), 7.22 (1H; **H**′5), 7.18 (1H; **H**8, **H**′10), 7.10 (2H; **H**′9), 7.00 (2H; **H**9), 6.95 (2H; **H**7), 6.94 (1H; **H**5), 6.90 (8H; *m*-C**H** of BPh_4), 6.85 (2H; **H**′7), 6.77 (4H; *p*-C**H** of BPh_4), 6.08 (1H; **H**′3), 5.99 (1H; **H**′4), 5.96 (2H; **H**6), 5.91 (2H; **H**′6), 5.86 (1H; **H**4), 5.38 (m, 1H; N′C**H**), 4.67 (br m; 1H, N**H**), 4.62 (m, 1H; NC**H**), 4.22 (m, 1H; N′C**H**), 4.12 (br m, 1H; N**H**), 3.84 (m, 1H; NC**H**), 2.87 (br m, 1H; N**H**CH_3), 2.44 (br d, 3H; NHC**H**$_3$), 2.28 (m, 1H; N′C**H**), 2.17 (m, 1H; PC**H**), 2.16 (m, 1H; N′C**H**), 2.00 ppm (m, 1H; PC**H**); ^{31}P{^{1}H} NMR (202 MHz, 298 K, $CDCl_3$): δ = 38.8 (d, ^2J(P,P) = 30.0 Hz; **P**Ph_2), 28.7 ppm (d, ^2J(P,P) = 30.0 Hz; **P**′Ph_2); ^{15}N{^{1}H} NMR (61 MHz, 298 K, $CDCl_3$): δ = 215.6 (**N**′1), 210.2 (**N**′2), 209.5 (**N**2), 209.4 (**N**1), 73.7 (d, J(P,N) = 32.8 Hz; -**N**H_2), 66.7 ppm (-**N**HCH_3); ^{13}C{^{1}H} NMR (150 MHz, 298 K, $CDCl_3$): δ = 164.1 (*i*-**C** of BPh_4), 148.0 (**C**3), 142.8 (**C**′3), 136.4 (**C**5), 135.8 (**C**′5), 135.7 (*o*-**C** of BPh_4), 133.1 (**C**′9), 130.6 (**C**9), 130.5 (**C**11), 129.9 (**C**6, **C**8, **C**′6), 129.3 (**C**′8), 129.2 (**C**10), 128.6 (**C**7), 128.0 (**C**′7, **C**′11), 127.1 (**C**′10), 125.4 (*m*-**C** of BPh_4), 121.5 (*p*-**C** of BPh_4), 106.3 (**C**′4), 105.9 (**C**4), 47.1 (N**C**H_2), 47.0 (N′**C**H_2), 43.1 (N**C**H_3), 23.8 (P**C**H_2), 25.0 ppm (P**C**H_2); ESIMS (DCM): *m*/*z* (%): 697.07 (100) [$RuCl(PyP)_2^+$]; elemental analysis calcd (%) for $C_{59}H_{60}BClN_6P_2Ru{\cdot}H_2O$: C 65.59, H 5.78, N 7.78; found: C 65.49, H 5.72, N, 8.03.

Crystallographic data: Empirical formula $C_{59}H_{60}BClN_6P_2Ru{\cdot}1.5(NH_2NHCH_3){\cdot}(CH_2)_4O$; M_r = 1203.62 g mol^{-1}; monoclinic; *C*2/*c*; V = 12603.6(10) Å^3; Z = 8; a = 30.2824(13), b = 10.8564(5), c = 38.948(2) Å; T = 200(2) K; $F(000)$ = 5048; β = 100.162(1)°; completeness 99.7%; θ range 2.63–25.00°; crystal size 0.31 × 0.14 × 0.04 mm; index ranges $-35 \geq h \geq 35$, $-12 \geq k \geq 12$, $-46 \geq l \geq 46$; reflns measured 76226, unique reflns 11054; R_{int} = 0.1492; GoF(all) = 1.063; R_1 [$I > 2\sigma(I)$] 0.0736; wR_2 [$I > 2\sigma(I)$] 0.1619; R_1 (all data) 0.1519; wR_2 (all data) 0.1836.

General procedure for all NMR spectroscopy scale reactions: Dried and degassed CD_2Cl_2 (0.6 mL) was transferred into a NMR tube fitted with a Young's valve that contained the bimetallic metal complex (**6** or **7**; ≈10 mg). The Young's valve was replaced with a rubber septum in either a N_2 or Ar glove-box. The dried and degassed substituted hydrazine (1,1-dimethylhydrazine, phenylhydrazine or *N*-aminopiperidine; ≈10 μL) was injected into the NMR tube by using an air-tight syringe. The rubber septum was quickly replaced by a Young's valve under a cone of Ar gas. The reaction was monitored by variable-temperature ^{1}H and ^{31}P{^{1}H} NMR spectroscopy. The ^{31}P{^{1}H} NMR spectroscopic data are given in Table 3.

Table 3. ^{31}P{^{1}H} NMR spectroscopic data for the products formed from the addition of phenylhydrazine, 1,1-dimethylhydrazine and *N*-aminopiperidine to **7** (CD_2Cl_2, 300 MHz, 250 K).

Substituted hydrazine	Product	$\delta_{^{31}P}$ [ppm][a]	^2J(P,P) [Hz]
phenylhydrazine	**10**	44.3, 33.4	33.7
1,1-dimethylhydrazine	**11**	37.5, 28.9	29.4
N-aminopiperidine	**12**	36.9, 29.3	30.0

[a] Both resonances are doublets.

Acknowledgements

Financial support from the Australian Research Council and the University of New South Wales is gratefully acknowledged. S.L.D. wishes to thank the Australian government for an Australian Postgraduate Award scholarship. J.W. acknowledges his postdoctoral scholarship from the German Academic Exchange Services (DAAD).

[1] D. V. Yandulov, R. R. Schrock, *Science* **2003**, *301*, 76–78.
[2] M. D. Fryzuk, S. A. Johnson, *Coord. Chem. Rev.* **2000**, *200–202*, 379–409.
[3] B. M. Barney, H.-I. Lee, P. C. Dos Santos, B. M. Hoffman, D. R. Dean, L. C. Seefeldt, *Dalton Trans.* **2006**, 2277–2284.
[4] B. K. Burgess, D. J. Lowe, *Chem. Rev.* **1996**, *96*, 2983–3011.
[5] G. Ertl, *Catalytic Ammonia Synthesis*, (Ed.: J. R. Jennings) Plenum, New York, **1991**, Chapter 3, pp. 109–132.
[6] B. T. Heaton, C. Jacob, P. Page, *Coord. Chem. Rev.* **1996**, *154*, 193–229.
[7] D. Sellmann, A. Hille, A. Rösler, F. W. Heinemann, M. Moll, G. Brehm, S. Schneider, M. Reiher, B. A. Hess, W. Bauer, *Chem. Eur. J.* **2004**, *10*, 819–830.
[8] S. Kuwata, Y. Mizobe, M. Hidai, *Inorg. Chem.* **1994**, *33*, 3619–3620.
[9] D. Sellmann, D. C. F. Blum, F. W. Heinemann, *Inorg. Chim. Acta* **2002**, *337*, 1–10.
[10] Q.-F. Zhang, H. Zheng, W.-Y. Wong, W.-T. Wong, W.-H. Leung, *Inorg. Chem.* **2000**, *39*, 5255–5264.
[11] G. Albertin, S. Antoniutti, M. Bortoluzzi, J. Castro-Fojo, S. Garcia-Fontan, *Inorg. Chem.* **2004**, *43*, 4511–4522.
[12] G. Albertin, S. Antoniutti, A. Bacchi, E. Bordignon, P. M. Dolcetti, G. Pelizzi, *J. Chem. Soc. Dalton Trans.* **1997**, 4435–4444.

[13] G. Albertin, S. Antoniutti, A. Bacchi, M. Bergamo, E. Bordignon, G. Pelizzi, *Inorg. Chem.* **1998**, *37*, 479–489.
[14] B. T. Heaton, C. Jacob, J. Ratnam, *Polyhedron* **1995**, *14*, 2677–2682.
[15] J. V. Barkley, B. T. Heaton, C. Jacob, R. Mageswaran, J. R. Sampanthar, *J. Chem. Soc. Dalton Trans.* **1998**, 697–701.
[16] G. Otting, B. A. Messerle, L. P. Soler, *J. Am. Chem. Soc.* **1996**, *118*, 5096–5102.
[17] G. Otting, B. A. Messerle, L. P. Soler, *J. Am. Chem. Soc.* **1997**, *119*, 5425–5434.
[18] G. Otting, L. P. Soler, B. A. Messerle, *J. Magn. Reson.* **1999**, *137*, 413–429.
[19] S. Vogel, A. Barth, G. Huttner, T. Klein, L. Zsolnai, R. Kremer, *Angew. Chem.* **1991**, *103*, 325–327; *Angew. Chem. Int. Ed. Engl.* **1991**, *30*, 303–304.
[20] R. R. Schrock, T. E. Glassman, M. G. Vale, M. Kol, *J. Am. Chem. Soc.* **1993**, *115*, 1760–1772.
[21] P. D. Frisch, M. M. Hunt, W. G. Kita, J. A. McCleverty, A. E. Rae, D. Seddon, D. Swann, J. William, *J. Chem. Soc. Dalton Trans.* **1979**, 1819–1830.
[22] M. G. Vale, R. R. Schrock, *Inorg. Chem.* **1993**, *32*, 2767–2772.
[23] T. E. Glassman, M. G. Vale, R. R. Schrock, *J. Am. Chem. Soc.* **1992**, *114*, 8098–8109.
[24] M. G. Vale, R. R. Schrock, *Organometallics* **1993**, *12*, 1140–1147.
[25] J. Bultitude, L. F. Larkworthy, D. C. Povey, G. W. Smith, J. R. Wilworth, G. J. Leigh, *J. Chem. Soc. Chem. Commun.* **1986**, 1748–1750.
[26] E. Sebe, M. J. Heeg, C. H. Winter, *Polyhedron* **2006**, *25*, 2109–2118.
[27] J. L. Crossland, L. N. Zakharov, D. R. Tyler, *Inorg. Chem.* **2007**, *46*, 10476–10478.
[28] L. D. Field, H. L. Li, S. J. Dalgarno, P. Turner, *Chem. Commun.* **2008**, 1680–1682.
[29] S. L. Dabb, B. A. Messerle, M. K. Smith, A. C. Willis, *Inorg. Chem.* **2008**, *47*, 3034–3044.
[30] R. M. Hunt, W. V. Hough, US Patent 3086016, **1963**.
[31] T. V. Ashworth, M. J. Nolte, E. Singleton, *J. Chem. Soc. Dalton Trans.* **1978**, 1040–1046.
[32] P. R. Srinivasan, R. L. Lichter, *J. Magn. Reson.* **1977**, *28*, 227–234.
[33] D. S. Wishart, C. G. Bigam, J. Yao, F. Abildgaard, J. Dyson, E. Oldfield, J. L. Markley, B. D. Sykes, *J. Biomol. NMR* **1995**, *6*, 135–140.
[34] T. D. Ferris, P. T. Lee, T. C. Farrar, *Magn. Reson. Chem.* **1997**, *35*, 571–576.
[35] D. Neuhaus, M. P. Williamson, *The Nuclear Overhauser Effect in Structure and Conformational Analysis*, Verlag Chemie, New York, **1989**.
[36] D. D. Perrin, W. L. F. Armarego, *Purification of Laboratory Chemicals, 3rd ed.*, Pergamon Press, Oxford, **1988**.
[37] A. Bax, M. Ikura, L. E. Kay, D. A. Torchia, R. Tschudin, *J. Magn. Reson.* **1990**, *86*, 304–318.

Received: June 2, 2008
Published online: September 18, 2008

